Altering the optoelectronic properties of neat and blended conjugated polymer films by controlling the process of film deposition

OTTO TODOR-BOER[a,b,c], IOAN PETROVAI[a,b], RALUCA TARCAN[a,b], ANA-MARIA CRACIUN[a], LEONTIN DAVID[b], SIMION BOGDAN ANGYUS[c], SIMION ASTILEAN[a,b], IOAN BOTIZ[a,*]
[a]*Interdisciplinary Research Institute in Bio-Nano-Sciences, Babes-Bolyai University, Treboniu Laurian 42, Cluj-Napoca 400271, Romania*
[b]*Faculty of Physics, Babes-Bolyai University, M. Kogalniceanu 1, 400084 Cluj-Napoca, Romania*
[c]*INCDO-INOE 2000, Research Institute for Analytical Instrumentation, Donath Street 67, 400293 Cluj-Napoca, Romania*

It is nowadays accepted that, when fabricating organic photovoltaics, special attention should be paid to the microstructure of the donor-acceptor active layers from nano- to microscale, as the optimization of molecular conformations in such layers can boost the optoelectronic properties. In this work, we compare neat films of poly[(5,6-difluoro-2,1,3-benzothiadiazol-4,7-diyl)-alt-(3,3'''-di(2-octyldodecyl)2,2';5',2'';5'',2''' quarter-thiophen-5,5'''-diyl)] conjugated polymer along with films blended with fullerene acceptors, that were deposited using both spin casting and convective self-assembly techniques. Our results show that convective self-assembly technique induces a more optimized film microstructure comprised of molecular conformations favoring a slightly higher photoluminescence quenching as well as shorter fluorescence lifetimes.

(Received May 29, 2019; accepted June 14, 2019)

Keywords: Conjugated polymers, Convective self-assembly, Fluorescence lifetime, Thin films microstructure, Photoluminescence quenching

1. Introduction

Nowadays, organic photovoltaics (OPVs) receive a great attention thanks to their highly desired properties such as flexibility, rather cheap production, lightweight or (semi)transparency [1-4], just to name a few. In the future OPVs could represent a viable solution to boost the renewable energy sector, especially that at the moment low cost casting processes such as slot die and inkjet speed up their production [5]. Moreover, in the last few years the power conversion efficiencies for organic solar cells exceeded 11% [6]. Solar cell efficiency is closely linked to the absorption capabilities of the active layer as well as to its microstructure at all length scales that essentially dictates the efficiencies of exciton diffusion, charge transfer at the donor-acceptor interfaces, carrier migration, etc. Achieving, for example, an active layer with optimized microstructure, that is comprised of appropriate molecular packing at the nanoscale, can facilitate better exciton splitting and charge transfer [7-11] and can lead to altered absorption and emission properties [12], including higher photoluminescence (PL) quenching [13-15].

There are many film-forming techniques that can be used to reach an optimized microstructure in the active layers, including spin casting [16], screen printing [17], inkjet printing [18], gravure printing [19] and coating [20], roll-to-roll techniques [21], knife-over-edge casting and meniscus coating [22], slot die coating [23], spray coating [24], etc. Each technique has its advantages and disadvantages. For example, some of these techniques are not being suited for high-volume production while others work with rather great losses of materials. Moreover, the morphology at nano- and micro-scale can be controlled and essentially optimized by choosing not only the most suitable deposition technique but, also the right experimental parameters [25]. Furthermore, controlling the fluid flow [26], using antisolvent and additives [27], controlling the evaporation rate [28], controlling the interactions between solute, solvent and substrate [29], etc., could further help optimizing film microstructure.

In this work we present the altering of the optoelectronic properties taking place in thin films of both neat poly[(5,6-difluoro-2,1,3-benzothiadiazol-4,7-diyl)-alt-(3,3'''-di(2-octyldodecyl)2,2';5',2'';5'',2''' quarter-thiophen-5,5'''-diyl)] (PCE11; see its chemical structure in Fig. 1a) and PCE11 blended either with [6,6]-phenyl-C61 butyric acid methyl ester ([C60]PCBM; Fig. 1b) or with [6,6]-phenyl C71 butyric acid methyl ester ([C70]PCBM; Fig. 1c) that were deposited using both spin casting and convective self-assembly (CSA) techniques. Note here that PCE11 is a low band-gap semiconducting polymer with a high crystallinity [30], good hole transport mobilities [31] and efficient light absorption [32] while fullerenes are considered in the literature as the most efficient electron acceptors in organic photovoltaic devices [33-35]. The results obtained using absorption, PL and fluorescence-lifetime imaging microscopy (FLIM) indicate that, in comparison to spin cast films, thin conjugated films deposited via CSA adopt more optimized molecular conformations that are slightly favoring PL quenching and thus, that could implicitly favor the charge transfer process in OPV devices [36]. Thus, CSA deposition technique can

be used to manipulate the optoelectronic properties in a highly reproducible manner over large area substrates.

2. Experimental section

PCE11 of a weight-average molecular weight $M_w = 112.707 kg/mol$, number-average molecular weight $M_n = 55.674 kg/mol$ and of Đ = 2.02 was purchased from Ossila Ltd, United Kingdom. [C70]PCBM (≥ 99%) and [C60]PCBM (≥ 99.5%) were acquired from Solenne BV, Netherlands.

Thin films of PCE11, PCE11:[C60]PCBM and PCE11:[C70]PCBM were prepared by spin casting at 2000 rpm (at room temperature) from a 6 g/l chlorobenzene solution previously heated at 80 °C for 1 hour, as well as by CSA at a deposition speed of 10 μm/s (at room temperature). Note that chlorobenzene is a good solvent for PCE11, [C60]PCBM and [C70]PCBM systems. A 50/50 weight % ratio was used to obtain blend solutions. For all films, regular microscopy cover glass was used as substrate. The CSA coater was comprised of a motorized translational stage that is using a linear actuator from Zaber Technologies and that is capable to move with speeds ranging between ~ 4.7 μm/s to 8 mm/s. A cover glass that acted as a blade was fixed in the near vicinity of the substrate at the desired angle while the polymer solution was placed on the substrate, underneath and nearby the edge of the blade. More details about this technique can also be found elsewhere [12].

Absorption spectra of thin films were acquired using a V-530 UV-VIS spectrophotometer from Jasco (spectral range of 190-1100 nm). PL spectra were collected using a FP-6500 spectrofluorometer from Jasco (excitation wavelength range of 220-750 nm). All PL spectra were recorded using an excitation wavelength of 640 nm.

FLIM measurements were performed on a MicroTime200 time-resolved confocal fluorescence microscope system (Pico-Quant), equipped with an inverted microscope (IX 71, Olympus) and coupled to a time-correlated single-photon counting module.

3. Results and discussions

We start by observing that FLIM technique was able to indirectly distinguish changes in microstructure, both in neat films of PCE11 and in PCE11:[C60]PCBM films, that were induced by spin casting and CSA deposition techniques (Fig. 2 a-b). This was possible due to the nature of FLIM images that were generated by determining the fluorescence lifetime for each pixel of a specific image. This means that a FLIM image represents a spatial map distribution of lifetimes of various excited chromophores. Thus, indirectly, FLIM images give information on film microstructure and on its inhomogeneities due to differences in fluorescence lifetimes generated by different speeds of energy transfer taking place, for example, in various structures/polymer chains adopting different molecular conformations. For example, in Fig. 2c we can notice that the histograms exhibiting the fluorescence lifetime for the neat PCE11 films deposited by spin casting and CSA are rather narrow, indicating, in average, a rather unique mechanism of decay, i.e. a unique lifetime corresponding to each of these films. That is why these films appeared rather featureless as it can be seen in Fig. 2a. Here, the as cast PCE11 film appeared smooth with only few scattered structures, while the film prepared using CSA exhibited slightly more structures homogeneously distributed over the whole area. But, plenty of such structures were visible for PCE11:[C60]PCBM films, with the observation that, the film deposited using CSA presented few additional larger aggregates (Fig. 2b).

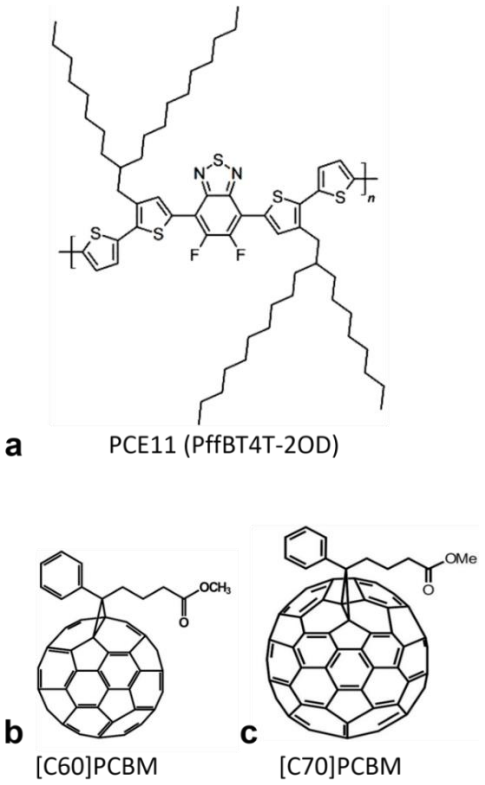

Fig. 1. (a-c) Molecular structure of electron donor PCE11 polymer (a) and electron acceptors [C60]PCBM (b) and [C70]PCBM (c).

Overall, the fluorescence average lifetime of the PCE11 film prepared by CSA appeared shorter (~ 0.35 ns) when compared to that recorded for the as cast film (~ 0.42 ns). Although not as clear, a similar trend was also observed for the two blended films. In this latter case, we could notice that the peak corresponding to the blended film made by spin casting was wider, most probably due to the existence of several types of intermixed morphologies. Furthermore, fluorescence lifetimes recorded for blended films were shorter than those measured for neat films, possibly indicating the existence of two different decaying mechanisms (for example, we do expect intense PL quenching to take place in blended films). According to the literature [37,38], shorter fluorescence lifetimes are corresponding to aggregates and/or to areas containing aggregated chains rather than to single chains. This

observation is in good agreement with our results which are showing more aggregates in blended films and in thin films deposited by CSA (Fig. 2 (a-b)).

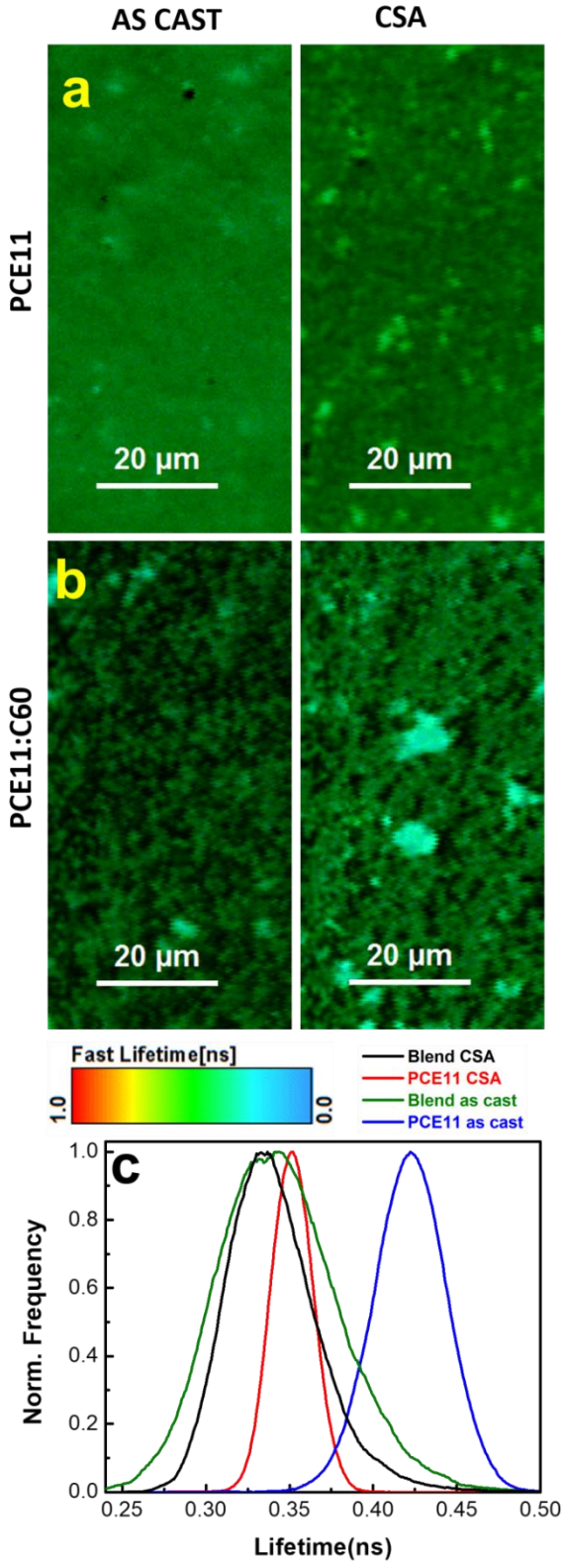

Fig. 2. (a-b) FLIM images of PCE11 (a) and PCE11:[C60]PCBM films (b) deposited by spin casting (left) as well as by CSA (right). (c) Normalized histograms of the corresponding fluorescence lifetimes

Because there is a demonstrated correlation between FLIM and PL quenching, both type of measurements being influenced by internal processes such as the exciton separation at the donor-acceptor interfaces, charge mobility and transfer [39, 40], we have further compared PL measurements of neat and blended films obtained by spin casting and CSA. Recorded results have shown that there is a significant PL quenching in both blended films, with the observation that PL quenching is higher (75%) in the film deposited using CSA compared to the as cast film (65%) (Fig. 3a). This most quenched PL intensity is corresponding to the shortest fluorescence lifetime (see the peak located at ~ 0.33 ns in Fig. 2c). This is in agreement with results reported in the literature for other donor-acceptor systems [41, 42]. We tentatively suggest that the 10% higher PL quenching observed in the CSA-cast film could be related to more favorable molecular conformations induced by CSA, i.e. to slightly smaller but probably more interconnected aggregates with larger interface area, that could enable stronger polymer-[C60]PCBM quencher interactions.

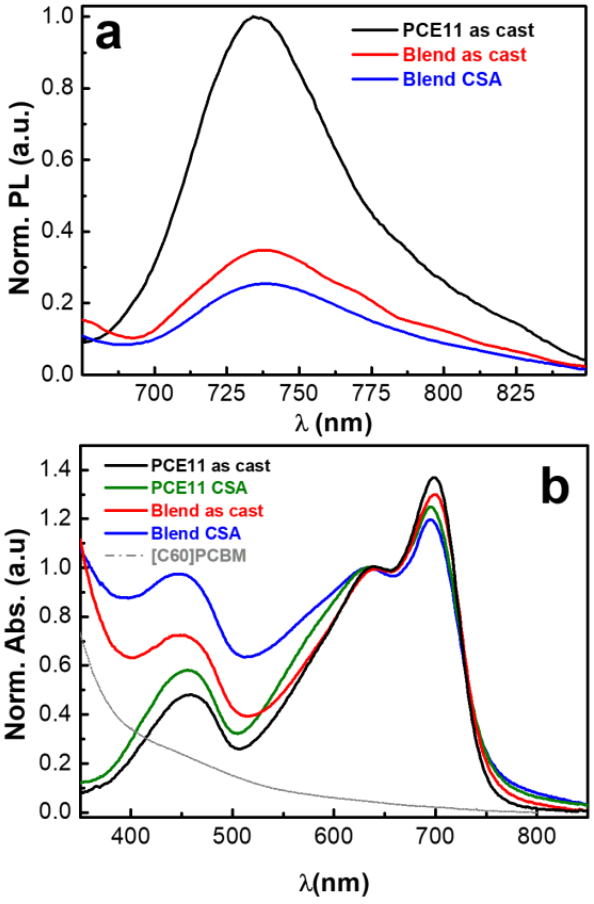

Fig. 3. (a-b) Normalized PL (a) and UV-VIS spectra (b) of PCE11 and PCE11:[C60]PCBM films obtained by spin casting and CSA

Changes on the molecular and supramolecular assembly level can further be inferred by comparing the absorption spectra of neat and blended films deposited by

spin casting and CSA. Indeed, the normalized absorption spectra presented in Fig. 3 b display several structure related features. We point out from the beginning that the presence of the three peaks located around 455 nm, 635 nm and 700 nm in the absorption spectra indicates the well-aggregated nature of PCE11 polymer system [43]. The peak located at ~ 700 nm is representing a strong 0-0 transition that is indicative of strong π-π interactions of the polymer chains in all films. This is in agreement to similar observations reported in the literature [34].

Moreover, in Fig. 3b we could observe that the intensity of 0-0 transition peak is slightly higher for the as cast films compared to the films obtained via CSA. This observation was also valid for neat films when compared to their corresponding blended films. Thus, we can conclude that both CSA technique as well as blending process are leading to films with slightly decreased aggregation and/or comprised of smaller π-π aggregates. We suggest this latter possibility to be more favorable as it is in line with our previous suggestion on the existence of smaller and rather more interconnected aggregates induced by CSA.

The above observations seem to be in contradiction with the FLIM results recorded for blended films and CSA-deposited films that exhibited shorter fluorescence lifetimes, an indicative of rather more aggregated structures (Fig. 2c). A possible explanation that would eliminate this contradiction could be the slightly different nature of the aggregates forming in our thin films. On one hand, neat films of highly crystalline PCE11 can display rather large aggregates of better molecular ordering given by a strong out-of-plane π–π stacking peak and more face-on orientation [34]. In comparison, films of PCE11 blended with fullerene tend to display still highly crystalline and yet ~ 30-40 nm small polymer domains [34]. On the other hand, it is not excluded that CSA could lead to smaller, but better interconnected aggregates than spin casting does due to the fact that CSA maintains constant the temperature of the substrate during unidirectional film deposition, which is not the case for spin casting.

The absorption results shown in Fig. 3b have furthermore revealed that the absorption of the PCE11:[C60]PCBM films was larger across the 350-630 nm spectral range (including the peak located at ~ 455 nm). This was attributed to the additional absorption of [C60]PCBM acceptor system (see the absorption of [C60]PCBM in Fig. 3b denoted by the broken grey line). This increase in light absorption by [C60]PCBM could eventually lead to the improvement of some specific parameters that are generally characterizing photovoltaic PCE11:[C60]PCBM devices [30].

All these previous results regarding PCE11 were further reconfirmed when we have blended this polymer system with the larger [C70]PCBM acceptor. Again, many aggregated structures were observed in FLIM images for both PCE11:[C70]PCBM films deposited using spin casting and CSA (Fig. 4a), with the observation that the structural features observed in the film deposited via CSA seemed finer and rather more interconnected. Moreover, fluorescence lifetime recorded for PCE11:[C70]PCBM as spin cast film was also shorter than that measured for its corresponding neat film (~ 0.36 ns compared to ~ 0.42 ns; see Fig. 4b). Similar trend was observed for blended and neat films deposited using CSA. Again, these results indicated that the microstructure of blended films and of thin films deposited using CSA is comprised of structures containing more aggregates[37, 38].

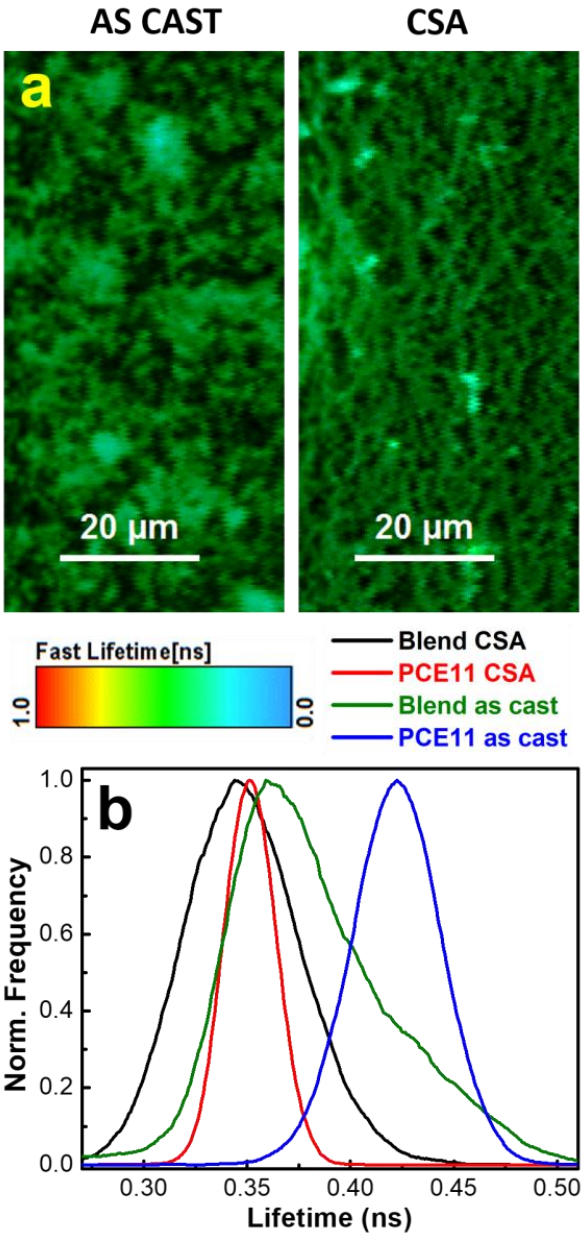

Fig. 4. (a) FLIM images of PCE11 and PCE11:[C70]PCBM films deposited using spin casting and CSA. (b) Normalized histograms of the corresponding fluorescence lifetimes

The emission and absorption properties of PCE11:[C70]PCBM films are presented in Fig. 5 and showed no notable differences when compared to those obtained for PCE11:[C60]PCBM films. PL quenching was still significant, reaching 68% and 62% for PCE11:[C70]PCBM films deposited using CSA and spin casting, respectively. These values are slightly lower than

those recorded for PCE11:[C60]PCBM films (see Fig. 3 a for comparison). Again, the most quenched PL intensity corresponded to the shortest average fluorescence lifetime of ~ 0.34 ns (see Fig. 4b).

Furthermore, the absorption spectra recorded for PCE11:[C70]PCBM films exhibited similar structural features given by the peaks located around 455 nm, 635 nm and 700 nm and thus, they pointed out towards the existence of a well-aggregated microstructure (Fig. 5b). In this case too, we could observe that the intensity of 0-0 transition peak located at ~ 700 nm was slightly higher for the as cast films compared to films obtained via CSA, most probably a direct consequence of the microstructure and of the degree of π-π aggregation induced by two very different methods of film deposition (see the rationale previously described for the PCE11:[C60]PCBM films). Again, the absorption of PCE11:[C70]PCBM films was larger across the 350-600 nm spectral range due to the additional absorption of [C70]PCBM (see its absorption spectrum indicated in Fig. 5b by the broken grey line).

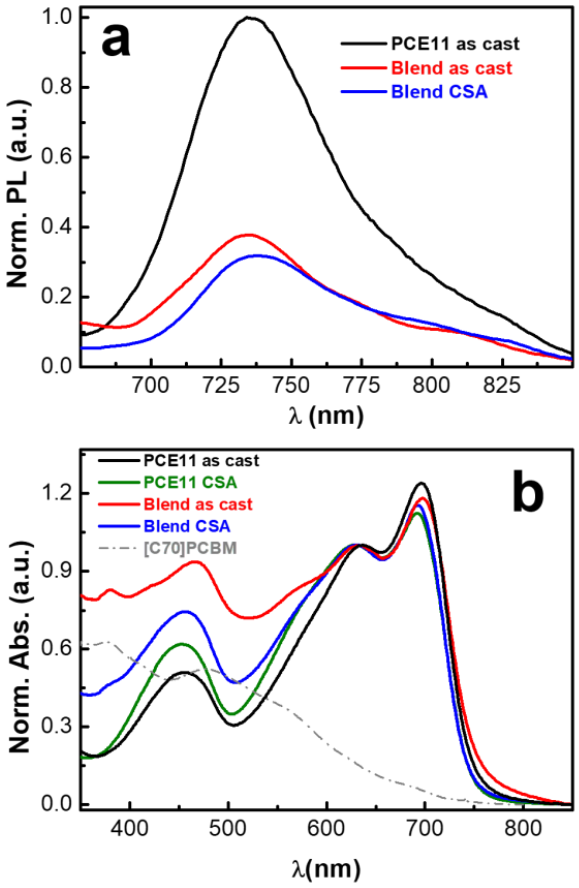

Fig. 5. (a-b) Normalized PL (a) and absorption (b) spectra of PCE11 and PCE11:[C70]PCBM films deposited by spin casting and CSA

4. Conclusions

In this work we have used CSA and spin casting deposition methods to obtain neat films of PCE11 as well as films blended with [C60]PCBM and [C70]PCBM fullerenes. We found a correlation between the film induced microstructure and the resulting optoelectronic properties such as absorption, emission or fluorescence lifetimes. In comparison to as spin cast films, films prepared by CSA technique exhibited slightly higher PL quenching and shorter fluorescence lifetimes due to more favorable molecular conformations and packing adopted by molecules during the deposition process. These results are valuable for the future design and fabrication of organic solar cells, with the emphasis on the processing of the active layers.

Acknowledgements

I. Botiz acknowledges the financial support of the Romanian National Authority for Scientific Research and Innovation, CNCS – UEFISCDI, project no. PN-II-RU-TE-2014-4-0013.

References

[1] T. Masuda, M. Inoue, J. Chantana, Y. Kudo, T. Minemoto, SAE Technical Paper 01-0863, 1 (2019)
[2] M. Tariq Saeed Chani, H. M. Marwani, E. Y. Danish, Kh. S. Karimov, M. Hilal, A. Hagfeldt, A.M. Asiri, J. Optoelectron. Adv. M. **19**, 178 (2017)
[3] M. Kaltenbrunner, M. S. White, E. D. Głowacki, T. Sekitani, T. Someya, N.S. Sariciftci, and S. Bauer, Nat. Commun. **3**, 770 (2012)
[4] J. Zhang, H.S. Tan, X. Guo, A. Facchetti, H. Yan, Nature Energy **3**, 720 (2018)
[5] C. L. Chochos, M. Spanos, A. Katsouras, E. Tatsi, S. Drakopoulou, V.G. Gregoriou, A. Avgeropoulos, Prog. Polym. Sci. **91**, 51 (2019)
[6] W. Zhao, S. Li, H. Yao, S. Zhang, Y. Zhang, B. Yang, and J. Hou, J. Am. Chem. Soc. **139**, 7148 (2017)
[7] P. Lee, W.-C. Li, B.-J. Chen, C.-W. Yang, C.-C. Chang, I. Botiz, G. Reiter, T.-L. Lin, J. Tang, A.C.-M. Yang, ACS Nano. **7**, 6658 (2013)
[8] Z. Gu, J. Guo, R. Hao, Z. Lin, Y. Qian, C. Ma, Y. Fan, X. Deng, G. Zhang, W. Peng, H. Xia, Q. Peng, and W. Zhu, Dyes and Pigments. **166**, 515 (2019)
[9] W. Chen, M. P. Nikiforov, S. B. Darling, Energy Environ. Sci. **5**, 8045 (2012)
[10] J. C. Bolinger, M. C. Traub, T. Adachi, P. F. Barbara, Science **331**, 565 (2011)
[11] Y. Guo, L. G. Wang, T. X. Zhang, D. L. Xie, J. Optoelectron. Adv. M. **20**, 624 (2018)
[12] I. Botiz, M.-A. Codescu, C. Farcau, C. Leordean, S. Astilean, C. Silva, and N. Stingelin, Journal of Materials Chemistry C **5**, 2513 (2017)
[13] W. Li, J. Cai, F. Cai, Y. Yan, H. Yi, R. S. Gurney, D. Liu, A. Iraqi, and T. Wang, Nano Energy **44**, 155 (2018)
[14] H. Cha, S. Wheeler, S. Holliday, S. D. Dimitrov,

A. Wadsworth, H. H. Lee, D. Baran, I. McCulloch, J. R. Durrant, Adv. Funct. Mater. **28**, 1704389 (2018)
[15] A. J. Cadby, R. Dean, C. Elliott, R. A. L. Jones, A. M. Fox, D.G. Lidzey, Adv. Mater. **19**, 107 (2007)
[16] D. M. DeLongchamp, B. M. Vogel, Y. Jung, M. C. Gurau, C. A. Richter, O. A. Kirillov, J. Obrzut, D. A. Fischer, S. Sambasivan, L. J. Richter, E. K. Lin, Chem. Mater. **17**, 5610 (2005)
[17] H. Zheng, Y. Zheng, N. Liu, N. Ai, Q. Wang, S. Wu, J. Zhou, D. Hu, S. Yu, S. Han, W. Xu, C. Luo, Y. Meng, Z. Jiang, Y. Chen, D. Li, F. Huang, J. Wang, J. Peng, Y. Cao, Nat. Commun. **4**, 1971 (2013)
[18] A. de la Fuente Vornbrock, D. Sung, H. Kang, R. Kitsomboonloha, V. Subramanian, Org. Electron. **11**, 2037 (2010)
[19] M. Hambsch, K. Reuter, M. Stanel, G. Schmidt, H. Kempa, U. Fügmann, U. Hahn, A. C. Hübler, Materials Science and Engineering: B **170**, 93 (2010)
[20] M. M. Voigt, R. C. I. Mackenzie, S. P. King, C. P. Yau, P. Atienzar, J. Dane, P. E. Keivanidis, I. Zadrazil, D. D. C. Bradley, J. Nelson, Sol. Energy Mater. Sol. Cells. **105**, 77 (2012)
[21] R. R. Søndergaard, M. Hösel, F. C. Krebs, J. Polym. Sci., Part B: Polym. Phys. **51**, 16 (2013)
[22] X. Gu, L. Shaw, K. Gu, M. F. Toney, Z. Bao, Nat. Commun. **9**, 534 (2018)
[23] L. Wengeler, B. Schmidt-Hansberg, K. Peters, P. Scharfer, W. Schabel, Chemical Engineering and Processing: Process Intensification. **50**, 478 (2011)
[24] G. Susanna, L. Salamandra, T. M. Brown, A. Di Carlo, F. Brunetti, A. Reale, Sol. Energy Mater. Sol. Cells. **95**, 1775 (2011)
[25] F. C. Krebs, Sol. Energy Mater. Sol. Cells. **93**, 394 (2009)
[26] T. Kawase, H. Sirringhaus, R. H. Friend, T. Shimoda, Adv. Mater. **13**, 1601 (2001).
[27] X. Liu, S. Huettner, Z. Rong, M. Sommer, R. H. Friend, Adv. Mater. **24**, 669 (2012).
[28] I. Botiz, N. Grozev, H. Schlaad, G. Reiter, Soft Matter. **4**, 993 (2008).
[29] Y. Diao, L. Shaw, Z. Bao, S. C. B. Mannsfeld, Energy Environ. Sci. **7**, 2145 (2014).
[30] Y. Zhang, A.J. Parnell, O. Blaszczyk, A. J. Musser, I. D. W. Samuel, D. G. Lidzey, G. Bernardo, Phys. Chem. Chem. Phys. **20**, 19023 (2018).
[31] R. Sharma, V. Gupta, H. Lee, K. Borse, R. Datt, C. Sharma, M. Kumar, S. Yoo, D. Gupta, Org. Electron. **62**, 441 (2018).
[32] X. Zhang, D. Zheng, S. Xing, H. Wang, J. Huang, J. Yu, Solar Energy. **147**, 106 (2017)
[33] F. Zhang, Z. Zhuo, J. Zhang, X. Wang, X. Xu, Z. Wang, Y. Xin, J. Wang, J. Wang, W. Tang, Z. Xu, Y. Wang, Sol. Energy Mater. Sol. Cells. **97**, 71 (2012)
[34] Y. Liu, J. Zhao, Z. Li, C. Mu, W. Ma, H. Hu, K. Jiang, H. Lin, H. Ade, H. Yan, Nat. Commun. **5**, 5293 (2014).
[35] A. T. Barrows, A. J. Pearson, C. K. Kwak, A. D. F. Dunbar, A. R. Buckley, D. G. Lidzey, Energy Environ. Sci. **7**, 2944 (2014).
[36] I. Botiz, S. B. Darling, Macromolecules **42**, 8211 (2009).
[37] L. A. Peteanu, G. A. Sherwood, J. H. Werner, A. P. Shreve, T. M. Smith, J. Wildeman, The Journal of Physical Chemistry C **115**, 15607 (2011).
[38] X.-T. Hao, L. J. McKimmie, T. A. Smith, The Journal of Physical Chemistry Letters **2**, 1520 (2011).
[39] Z. Xu, H. Tsai, H.-L. Wang, M. Cotlet, The Journal of Physical Chemistry B **114**, 11746 (2010).
[40] H. Tsai, Z. Xu, R. K. Pai, L. Wang, A. M. Dattelbaum, A. P. Shreve, H.-L. Wang, M. Cotlet, Chem. Mater. **23**, 759 (2011).
[41] Y. Wang, D. Kurunthu, G. W. Scott, C. J. Bardeen, The Journal of Physical Chemistry C **114**, 4153 (2010).
[42] Y.-Y. Lin, C.-W. Chen, J. Chang, T Y. Lin, I S. Liu, W.-F. Su, Exciton dissociation and migration in enhanced order conjugated polymer/nanoparticle hybrid materials, Nanotechnology **17**, 1260 (2006).
[43] W. Ma, G. Yang, K. Jiang, J. H. Carpenter, Y. Wu, X. Meng, T. McAfee, J. Zhao, C. Zhu, C. Wang, H. Ade, H. Yan, Advanced Energy Materials **5**, 1501400 (2015).

*Corresponding author: ioan.botiz@ubbcluj.ro